

Transition to chaos by interaction of resonances in dissipative systems. I. Circle maps

Mogens Høgh Jensen

H. C. Ørsted Institute, Universitetsparken 5, DK-2100 Copenhagen Ø, Denmark

Per Bak

Physics Department, Brookhaven National Laboratory, Upton, New York 11973

Tomas Bohr

Laboratory of Atomic and Solid State Physics, Cornell University, Ithaca, New York 14853

(Received 9 May 1984)

Dissipative dynamical systems with two competing frequencies exhibit transitions to chaos. We have investigated the transition through a study of discrete maps of the circle onto itself. The transition is caused by interaction and overlap of mode-locked resonances and occurs at a critical line where the map loses invertibility. At this line the mode-locked intervals trace up a complete devil's staircase whose complementary set is a Cantor set with fractal dimension $D \sim 0.87$. Numerical results indicate that the dimension is universal for maps with cubic inflection points. Below criticality the staircase is incomplete, leaving room for quasiperiodic behavior. The Lebesgue measure of the quasiperiodic orbits seems to be given by an exponent $\beta \sim 0.35$ which can be related to D through the scaling relation $D = 1 - \beta/\nu$. The exponent ν characterizes the cutoff of narrow plateaus near the transition. A variety of other exponents describing the transition to chaos is defined and estimated numerically.

I. INTRODUCTION

Our quantitative knowledge about highly nonlinear dynamical systems is very meager. In a few cases exact solution of the dynamical equations exist, but their behavior is atypical—the very possibility of obtaining analytical solutions excludes the occurrence of chaotic motion which is of importance in any “truly” nonlinear system. A major breakthrough came—especially through the work of Feigenbaum¹—with the realization that one-dimensional maps are an important laboratory for nonlinear studies. Not only do these maps qualitatively model the kinds of behavior found in dynamical systems, but, more astonishingly, scaling behavior found in the maps carry quantitatively over to real systems.

In this paper and the following one (denoted II) we shall study scaling behavior for one-dimensional circle maps and show that the same scaling exponents can be found in dissipative dynamical systems that exhibit mode locking. Mode locking is a resonant response occurring in systems of coupled oscillators or oscillators coupled to periodic external forces. In general, resonances occur whenever the frequency of a harmonic, $P\omega_1$, of one oscillator approaches some harmonic, $Q\omega_2$, of another; and in the resonant region the frequencies of the two oscillators locks exactly into the rational ratio P/Q .

The mechanism, in these systems, leading eventually to chaotic behavior is interactions between the different resonances, caused by the nonlinear couplings, and overlap between the resonant regions when the couplings exceed a certain critical value. In some sense the mechanism is the analog, for dissipative systems, of Chirikov's instability of quasiperiodic orbits in Hamiltonian systems.²

In II some specific systems from condensed-matter physics (Josephson junctions in microwave fields, charge-density waves in periodic electric fields) and from classical mechanics (the “swing” or the damped driven pendulum) will be considered. The main result is that the behavior of these systems, including the transition to chaos, can be described by one-dimensional discrete maps of the circle onto itself, the so-called “circle maps,” which is the subject of this paper. In general, circle maps are defined through

$$\theta_{n+1} = f_{\Omega}(\theta_n) = \theta_n + \Omega + g(\theta_n), \quad (1.1)$$

where

$$g(\theta_n) = g(\theta_n + 1) \pmod{1} \quad (1.2)$$

and can thus be thought of as “lifts” of mappings from the circle to itself. The advantage of studying simple maps on this form is obvious. It is much easier to identify periodic, quasiperiodic, and chaotic solutions by iterating the map than by a cumbersome numerical integration of the underlying differential equation. The variables θ_n represent the phase of the oscillating system measured stroboscopically at periodic time intervals $t_n = 2\pi n / \omega_2$, using the frequency of the external force, or one of the oscillating parts as a clock. A phase shift $\theta_n \rightarrow \theta_n + 1$ represents a full rotation; hence the periodic property (1.2) of g . The map has a linear term θ_n and a bias term Ω representing the frequency of the system in the absence of the nonlinear coupling g .

To study the mode locking in the circle map we consider iterations of the map, θ , $f(\theta)$, $f^2(\theta)$, \dots , or θ_1 , θ_2 , θ_3 , \dots . The iteration of the map is conveniently described by the winding number

$$W = \lim_{n \rightarrow \infty} [(f_{\Omega}^n - \theta)/n]. \quad (1.3)$$

The winding number is the mean number of rotations per iteration, i.e., the frequency of the underlying dynamical system, so $W = \Omega$ in the absence of the nonlinear coupling. Under iteration the variable θ_n may converge to a series which is either *periodic*, $\theta_{n+Q} = \theta_n + P$, with rational winding number $W = P/Q$; *quasiperiodic*, with irrational winding number $W = q$; or *chaotic* where the series behaves irregularly.

Although the question of the existence of smooth behavior in circle maps has very much the flavor of the general problem of the existence of smooth invariant tori in dynamical systems [the Kolmogorov-Arnol'd-Moser (KAM) problem], much stronger theorems³ due to Arnol'd⁴ and Herman⁵ hold for the one-dimensional circle maps. As long as $f(\theta)$ is a diffeomorphism, i.e., smooth and invertible, these theorems guarantee that no chaotic motion can occur.

The nontrivial scaling behavior that we shall discuss occurs precisely at the point (subsequently denoted the critical point) in parameter space where $f(\theta)$ loses its invertibility. In that case the theorems mentioned above break down and not much is known in general. The first exposition of interesting scaling behavior at the critical point was given in a numerical investigation by Shenker⁶ followed by renormalization-group treatments by Feigenbaum, Kadanoff, and Shenker⁷ and by Rand, Ostlund, Sethna, and Siggia.⁸ These studies concentrated on specific well-behaved winding numbers—mostly on the “golden mean,” $(\sqrt{5}-1)/2$ —and showed that nontrivial scaling behavior is found when the golden mean is approached through a sequence of rational winding numbers.

In our work we have generalized these ideas and asked for the global scaling properties of the mode-locking pattern. From the outset it was not clear whether any simple universal properties should exist globally since the renormalization-group treatments^{7,8} are only valid for a measure-zero set of winding numbers. We do, however, find strong numerical evidence for nontrivial scaling behavior, and from this we can derive general universal “average” exponents distinctly different from their golden-mean values. A short account of these findings has already been published.⁹

Most of our results are obtained for the sine map

$$\theta_{n+1} = f_{\Omega}(\theta_n) = \theta_n + \Omega - (K/2\pi)\sin 2\pi\theta_n, \quad (1.4)$$

but in order to check universality we have also investigated maps in which the sine function has been replaced by higher-order polynomials (Sec. IV).

The mapping (1.4) is sketched in Fig. 1(a) for $\Omega = 0.2$ and $K = 0.9$. Because of the periodicity of the map we have reduced it to the square $0 \leq \theta_n < 1$, $0 \leq \theta_{n+1} < 1$. We see two branches in the unit square. When $K < 1$ the map is strictly monotonic. At $K = 1$ [Fig. 1(b)] the map develops a cubic inflection point at $\theta = 0$, so the map is still invertible but the inverse map has a singularity. For $K > 1$ [Fig. 1(c)] the map develops a local maximum and a local minimum and is no longer invertible. The figure shows a chaotic trajectory.

We shall here be concentrating on the situation for K

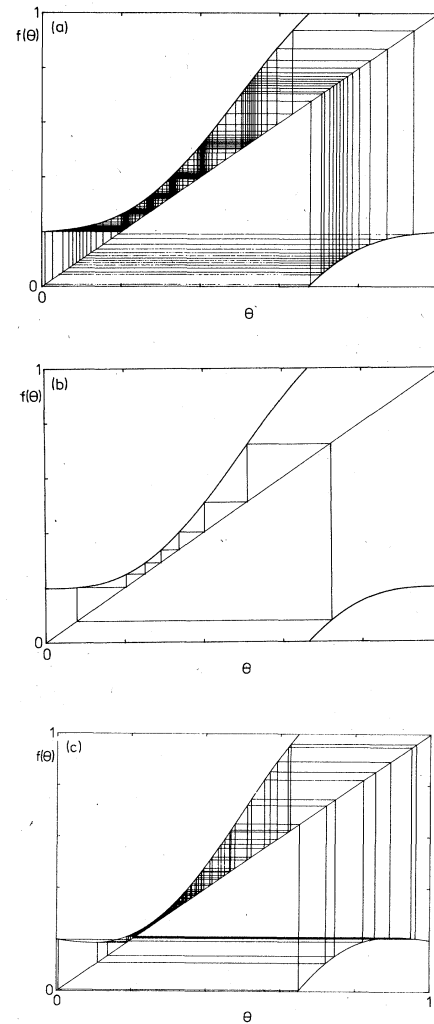


FIG. 1. Evolution of iterations of the circle map (1.3) for $\Omega = 0.2$ and (a) $K = 0.9$, (b) $K = 1.0$, and (c) $K = 1.1$. For $K > 1$ the map develops local maxima (and minima) and chaotic behavior may occur.

equal to or slightly below 1. For $0 < K < 1$ it has been shown⁵ that the winding number locks-in at every single rational number P/Q in a nonzero interval of Ω , $\Delta\Omega(P/Q)$. For K close to zero all intervals are quite small so the probability that the winding number for a random value of Ω is rational is almost zero, i.e., the probability of hitting an irrational winding number is almost one. However, with increasing K the widths of all the phase-locked intervals increase (Fig. 2), so for $K = \frac{1}{2}$ the probabilities of observing rational and irrational winding numbers are almost equal. For $K \sim 1$ the probability of finding a rational winding number is close to 1. The regimes in (Ω, K) space where W assumes rational values are called “Arnol'd tongues.” Clearly, the widths of the resonances cannot grow indefinitely: at some point they will overlap. It will be shown numerically that at $K = 1$ the resonances will completely fill up the critical line, confining the quasiperiodic orbits to a Cantor set of zero measure.

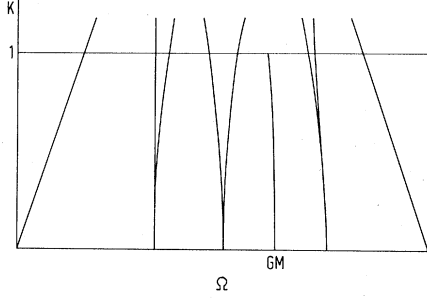


FIG. 2. Schematic phase diagram for circle map in (Ω, K) space. Note the Arnol'd tongues where the winding number assumes locked rational values. The winding number assumes irrational values (such as the golden mean) along one-dimensional curves ending at $K=1$.

Let us briefly summarize our findings. Figure 3 shows the winding number as a function of Ω at $K=1$. The plateaus in this function forms a complete "devil's staircase," a structure which has previously been found in quite different contexts, such as the one-dimensional Ising model with long-range interactions,¹⁰ the Frenkel-Kontorowa model of atoms adsorbed on a periodic substrate,¹¹ and the three-dimensional (3D) Ising model with competing interactions.¹²

The complementary set (on the Ω axis) to a complete staircase is a Cantor set of fractal dimension $D \leq 1$. For the staircase of the circle map we find $D \sim 0.87$; this number is the universal index characterizing the transition to chaos by mode locking.

For $K < 1$ the staircase is no longer complete; there is room for quasiperiodic orbits. Near $K=1$ we find that the integrated measure M of the quasiperiodic orbits is described by an exponent β :

$$M \sim (1-K)^\beta, \quad (1.5)$$

where β is related to the fractal dimension D through the scaling law $D=1-\beta/\nu$. Here, ν is an exponent characterizing the cutoff of narrow plateaus versus $(1-K)$, i.e., ν is the exponent for the crossover between the critical behavior with $D \sim 0.87$ at the transition and the regular behavior with $D=1$ below the transition. Hence, below criticality the resonances are separated by quasiperiodic orbits, at criticality the resonances fill up the critical line,

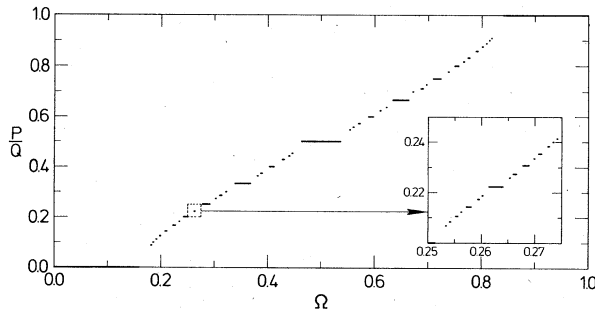


FIG. 3. Winding number W vs Ω for the circle map at $K=1$. Steps with $\Delta(P/Q) > 0.0015$ are shown. The inset shows intervals with $\Delta > 0.00015$. Note the self-similar nature of the staircase under magnification.

and above criticality the resonances overlap. The chaos occurring in the supercritical region is a "frustrated" response of the system due to the overlaps: the orbit jumps between resonances in an erratic way.

The remaining part of the paper is organized as follows. In Sec. II we present the numerical methods; in Sec. III the scaling of resonances at the critical line is investigated for the sine circle map. In Sec. IV the universality conjecture is tested by investigating circle maps with different periodic functions. In Sec. V additional critical exponents are defined and derived; in particular, we calculate the exponent β characterizing the integrated Lebesgue measure of the quasiperiodic orbits below criticality. Finally, in Sec. VI the scaling near rational winding numbers is investigated.

II. NUMERICAL METHODS

In order to find the widths of the various resonances $\Delta\Omega(P/Q)$ we consider the stability of an orbit with rational winding number. The cycle $\theta_1, \theta_2, \dots, \theta_Q$ ($=\theta_1+P$), with period Q is stable as long as

$$\frac{df_\Omega^Q(\theta_i)}{d\theta_i} = \prod_{i=1}^Q f'_\Omega(\theta_i) < 1. \quad (2.1)$$

Thus, the endpoints of the plateaus are determined by the condition $df_\Omega^Q(\theta_i)/d\theta_i=1$, together with the condition $f_\Omega^Q(\theta_i)=\theta_i+P$. From the condition $f(\theta^*)=\theta^*$ and $f'(\theta^*)=1$, we find analytically that

$$\Delta\Omega(0/1) = (-K/2\pi, K/2\pi)$$

for the map (1.7). The stability of a general P/Q step is found by a two-dimensional Newton iteration method. We define the functions

$$\begin{aligned} g_1(\theta, \Omega) &= f_\Omega^Q(\theta) - \theta - P, \\ g_2(\theta, \Omega) &= \frac{df_\Omega^Q(\theta)}{d\Omega} - 1, \end{aligned} \quad (2.2)$$

or

$$\vec{g}(\theta, \Omega) = \begin{bmatrix} g_1(\theta, \Omega) \\ g_2(\theta, \Omega) \end{bmatrix}.$$

The stability criteria can be expressed simply as $\vec{g}(\theta^*, \Omega^*) = \vec{g}^* = \vec{0}$. Expanding \vec{g}^* around the initial point of the iteration, $\vec{g}(\theta^0, \Omega^0) = \vec{g}_0$,

$$\vec{g}^* \simeq \vec{g}_0 + \vec{\Delta} \vec{M}, \quad (2.3)$$

where

$$\vec{\Delta} = (\theta^*, \Omega^*) - (\theta^0, \Omega^0) \quad (2.4a)$$

and

$$\vec{M} = \begin{bmatrix} \frac{\partial g_1}{\partial \theta} & \frac{\partial g_1}{\partial \Omega} \\ \frac{\partial g_2}{\partial \theta} & \frac{\partial g_2}{\partial \Omega} \end{bmatrix}, \quad (2.4b)$$

we find (for $\vec{g}^* = \vec{0}$)

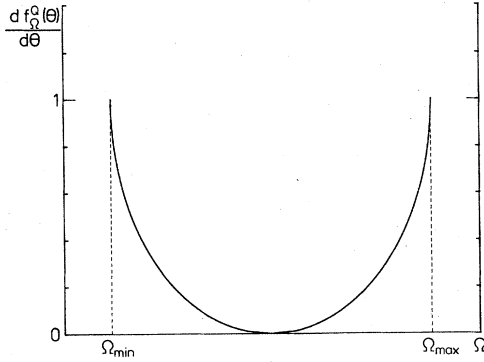


FIG. 4. $F'(\theta_i) = \prod_{i=1}^Q f'_{\Omega}(\theta_i)$ within the stability interval for the periodic orbit with $W = P/Q = \frac{2}{9}$.

$$\vec{\Delta} \simeq -\underline{M}^{-1} \vec{g}_0, \quad (2.5)$$

and so, as the first approximation,

$$(\theta^*, \Omega^*) \simeq (\theta^1, \Omega^1) = -\underline{M}^{-1} \vec{g}_0 + (\theta^0, \Omega^0). \quad (2.6)$$

Iterating the equations (2.5) and (2.6), it is possible to locate the endpoints of a P/Q interval even when Q is very large ($Q \sim 4000$). Note that all derivatives can be derived recursively

$$\begin{aligned} \frac{\partial f_{\Omega}^{i+1}(\theta)}{\partial \theta} &= [1 - K \cos(2\pi\theta_i)] \frac{\partial f_{\Omega}^i(\theta)}{\partial \theta}, \\ \frac{\partial^2 f_{\Omega}^{i+1}(\theta)}{\partial \Omega \partial \theta} &= 2\pi K \sin(2\pi\theta_i) \frac{\partial f_{\Omega}^i(\theta)}{\partial \theta} \frac{\partial f_{\Omega}^i(\theta)}{\partial \Omega} \\ &\quad + [1 - K \cos(2\pi\theta_i)] \frac{\partial^2 f_{\Omega}^i(\theta)}{\partial \Omega \partial \theta}. \end{aligned} \quad (2.7)$$

To initiate the iteration it is always convenient to locate the superstable point $(\theta, \Omega) = (\theta_s, \Omega_s)$, where $df_{\Omega_s}^Q(\theta_s)/d\theta = 0$. At $K=1$, $\theta_s=0$ and Ω_s is determined by $f_{\Omega_s}^Q(0) = P$. This point is always close to the midpoint of the interval. Figure 4 shows the variation of $df_{\Omega}^Q(\theta)/d\theta$ within the stability interval. This function has infinite slope at the end points of the interval and is close to a half-ellipse.

With this numerical method we have found all intervals with $0 < P/Q < \frac{1}{2}$ and $Q \leq 95$ giving 1388 intervals $\Delta(P/Q)$ in the range between 0.3 and 0.000002. All steps were found to an accuracy of 10^{-8} . Due to the symmetry of the map (1.4) as $\theta \rightarrow -\theta$, the staircase is symmetric around $\Omega = \frac{1}{2}$, so $\Delta(P/Q) = \Delta(1 - P/Q)$.

III. SCALING OF THE STAIRCASE AT THE TRANSITION TO CHAOS

All the intervals with $Q \leq 95$ were found to be stable in a nonzero interval for $K=1$. Figure 5 shows the widths of the steps $\Delta(P/Q)$ versus P/Q . Note the self-similarity of the function under rescaling. We conjecture that eventually $\Delta(P/Q) > 0$ for all P and all Q . By including more and more steps, with higher Q and smaller widths the Ω axis becomes more and more "filled up." This is not different from the situation for $K < 1$.⁴

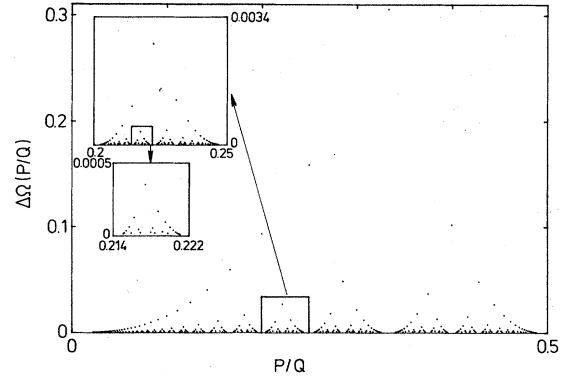


FIG. 5. $\Delta(P/Q)$ vs P/Q . Note the self-similarity of the diagram under scaling.

However, one might speculate that eventually the mode-locked intervals will cover the entire Ω axis. In this case the staircase is called *complete*. To investigate whether or not this is the case we have calculated the total width $S(r)$ of all steps which are larger than a given scale r . We are interested in the space between the steps, $1 - S(r)$, and have measured it on the scale r to find the "number of holes," $N(r) = [1 - S(r)]/r$. Here the Ω interval is of length 1, in general, the interval may have any length Ω_0 and the number of holes is $N(r) = [\Omega_0 - S(r)]/r$. In Fig. 6 $\log_{10} N(r)$ has been plotted versus $\log_{10} 1/r$ for 40 values of r in the interval (0.0009, 0.000017). The points fall excellently on a straight line indicating a power law

$$N(r) \sim \left(\frac{1}{r} \right)^D. \quad (3.1)$$

From the slope of the straight line we find $D = 0.8700 \pm 3.7 \times 10^{-4}$. The uncertainty on D was found from a standard linear regression analysis. The result (3.1) means that the space between the steps vanishes as

$$1 - S(r) \sim r^{1-D} \quad (3.2)$$

as $r \rightarrow 0$. We, therefore, conjecture that the staircase is *complete*. The exponent D is the fractal dimension¹³ of

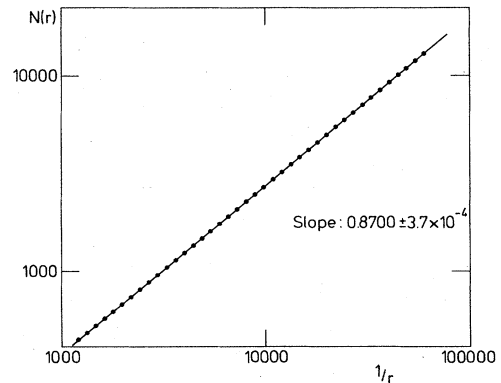


FIG. 6. Plot of $\log_{10} N(r)$ vs $\log_{10} (1/r)$ for the critical circle map. The slope of the straight line yields $D = 0.8700 \pm 3.7 \times 10^{-4}$.

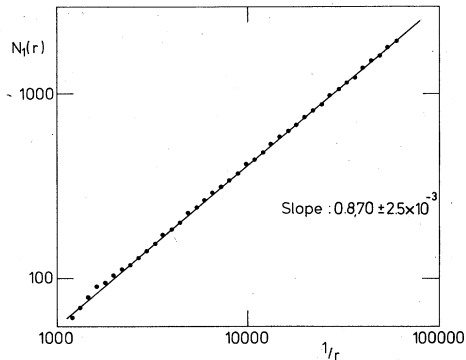


FIG. 7. Plot of $\log_{10}N_1(r)$ vs $\log_{10}(1/r)$ for the critical circle map. The slope of the line yields $D_1=0.870\pm 2.5\times 10^{-3}\simeq D$.

the staircase, or rather the fractal dimension of the Cantor set of zero Lebesgue measure which is the complementary set to the mode-locked intervals on the Ω axis.

The fractal dimension can be determined by an alternative method by simply counting the number of steps $N_1(r)$ which are larger than a given scale r .¹⁰ This number is given by the equation

$$\frac{\partial N_1}{\partial r} = -\frac{1}{r} \frac{\partial S(r)}{\partial r} \sim -\frac{1}{r} \frac{\partial r^{1-D}}{\partial r} \sim r^{-1-D}, \quad (3.3)$$

so the total number of steps wider than r is

$$N_1(r) = \int_r^{r_0} \frac{\partial N_1}{\partial r} dr = r^{-D} + \text{const}. \quad (3.4)$$

To investigate whether or not N_1 fulfills the condition (3.4), we have counted $N_1(r)$ for several values of r . Figure 7 shows $\log_{10}N_1(r)$ plotted versus $\log_{10}(1/r)$. Again

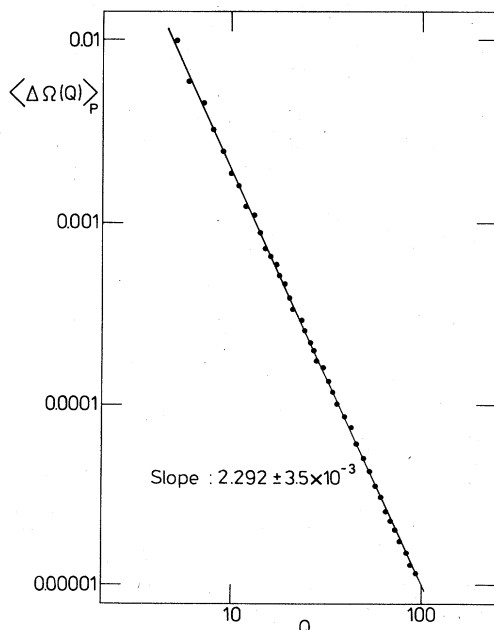


FIG. 8. Plot of $\log_{10}\langle \Delta\Omega(Q) \rangle_P$ vs Q . The slope of the line yields $\delta=2.292\pm 3.4\times 10^{-3}$.

the points fall on a straight line so

$$N_1(r) \sim \left(\frac{1}{r}\right)^{D_1} \quad (3.5)$$

with $D_1=0.870\pm 2.5\times 10^{-3}\simeq D$ as it should be. The latter method seems easier to use when analyzing experiments since uncertainties in the determination of the stepwidth are not accumulated as when $S(r)$ is calculated. On the other hand, even if $N_1(r)$ obeys the simple power law (3.5) there is no guarantee that the staircase is complete. Integration of (3.5) leads to

$$S(r) \sim r^{1-D} + C,$$

where C is an integration constant. Thus, the power law (3.5) does not rule out a finite probability $\sim(1-C)$ of quasiperiodic orbits, so the two methods are equivalent only when the staircase is known to be complete.

Another dimension D_2 can be calculated as follows. The mean values of steps with a given denominator Q , $\langle \Delta\Omega(Q) \rangle_P$, can be found by averaging over the numerator P . Figure 8 shows $\log_{10}\langle \Delta\Omega(Q) \rangle_P$ versus $\log_{10}Q$, again indicating a power-law behavior,

$$r_Q = \langle \Delta\Omega(Q) \rangle_P \sim Q^{-\delta} \quad (3.6)$$

with $\delta=2.292\pm 3.4\times 10^{-3}$. The exponent δ is related to a dimension D_2 in the following way. The number of rationals with denominator Q_0 is approximately $(3/\pi^2)Q_0$. The total number of rationals with denominator smaller than Q_0 is thus

$$N_0 \sim \int_1^{Q_0} Q dQ \sim Q_0^2$$

and D_2 is defined as

$$D_2 = \frac{\log_{10}N_0}{\log_{10}1/r_0} = \frac{2 \log_{10}Q_0}{\delta \log_{10}Q_0} = \frac{2}{\delta} = 0.873 \pm 2.1 \times 10^{-3}. \quad (3.7)$$

We stress that since $\Delta(P/Q)$ is a function of both P and Q , not only of Q , it is not a mathematical necessity that $D_2=D$; it is not even a certainty that D_2 is well defined even if D is. However, our numerical results are consistent with D_2 being identical to D .

For intervals $\Delta(P_i/P_{i+1})$, where P_i are Fibonacci numbers, converging to the inverse golden-mean winding number, Shenker⁶ found

$$\Delta(P/Q) \sim Q^{-\delta'}, \quad \delta' \simeq 2.16,$$

so the average exponent found from (3.6) is distinctly different.

When passing beyond the $K=1$ line the steps continue to increase. Since they fill up the whole Ω axis for $K=1$, they must necessarily overlap for $K>1$ (see Fig. 9). In an experimental situation, the transition to chaos is most easily identified by considering hysteresis involving the smallest steps. As soon as two steps overlap, an infinity of smaller steps in between are squeezed out. The overlap regimes correspond to chaotic or hysteretic solutions. The "in between" steps yield an infinity of metastable solu-

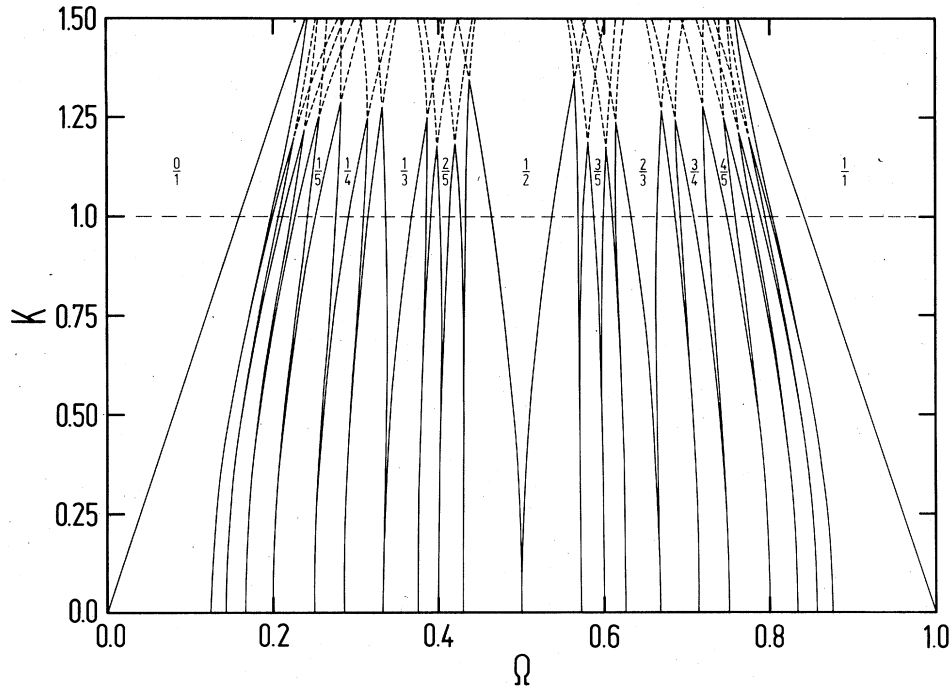


FIG. 9. Phase diagram for the sine circle map. The dotted lines indicate overlap of resonances.

tions which may all be observed in a numerical iteration process just by varying the initial point θ_0 . Chaotic behavior arises because the orbit jumps between the various overlapping resonances in an erratic way. *The transition to chaos is caused by overlap of resonances.* A transition of this type has been observed in a variety of physical systems as for instance Josephson junctions in microwave fields¹⁴ and sliding charge-density waves,¹⁵ we will discuss these systems in the following paper. Most nonlinear periodic systems perturbed by an external periodic field (sinusoidal or pulsed) will probably exhibit a transition to chaos caused by overlap of resonances as described here.

For $K > 1$ the map develops quadratic maxima and minima. It is well known from the work of Feigenbaum¹ that iterations of this type of mapping exhibit infinite series of period doubling leading to chaos. This type of chaos (associated with instabilities near the superstable points—not the edges of the steps) has been studied in detail by Glass and Perez¹⁶ and by Kaneko.¹⁷ Bifurcations of a P/Q cycle lead to the cycles $2P/2Q$, $4P/4Q$, $8P/8Q$, . . . , so the winding number is unaffected.

IV. UNIVERSALITY

It is important to know whether or not the critical behavior at the transition to chaos is “universal,” i.e., whether or not it depends on the specific function $f(\theta)$ in (1.1). In an experiment we do not know the function $f(\theta)$, and it is unlikely that it is a simple sine function (see the following paper). For the theory here to be *predictive* in such cases it is imperative that the critical behavior is universal. To check the universality of the scaling dimension $D \sim 0.87$, we have studied a class of mappings

$$f_{\Omega,a}(\theta) = \theta + \Omega - (K/2\pi)[\sin(2\pi\theta) + a \sin^3(2\pi\theta)]. \quad (4.1)$$

For $-\frac{4}{3} < a < \frac{1}{6}$ the function f is monotonic and has a cubic inflection point at $\theta=0$. Generally, the details of the staircases are different from the staircase shown in Fig. 3. Some steps become wider, some become narrower. The scaling behavior, however, remains the same, independently of a . Figure 10 shows $\log_{10}[1-S(r)/r]$ versus $\log_{10}(1/r)$ for $a = -0.8$, -0.25 , and 0.15 . The points for $a=0.15$ seemingly exhibit a crossover from $D \sim 0.81$ to $D \sim 0.87$. We shall return to this point shortly. Again we find that the points fall on a straight line with slope $D=0.870$. The staircases of the maps (4.1)

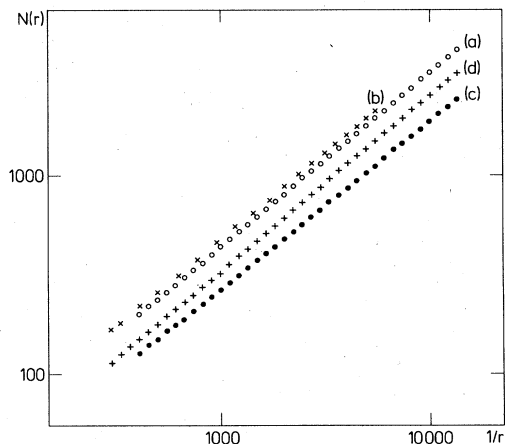


FIG. 10. $\log_{10}N(r)$ vs $\log_{10}(1/r)$ for the map (4.1) with (a) $a = -0.25$, (b) $a = -0.8$, and (c) $a = 0.15$, and for the map (4.2) with (d) $b = 0.2$.

also obey the symmetry $\Delta(P/Q) = \Delta(1 - P/Q)$. In order to check that this symmetry does not influence the fractal dimension, we have studied the map

$$f_{\Omega,b}(\theta) = \theta + \Omega - (K/2\pi)[\sin(2\pi\theta) + b \sin^4(2\pi\theta)] \quad (4.2)$$

for $b=0.2$ and $K=1$. Due to the even term the staircase is not symmetric but it is still complete with $D \sim 0.87$ [see Fig. 10(d)].

From these investigations we conjecture that staircases constructed from maps with cubic inflection points are complete with a universal fractal dimension 0.87. This number is thus a universal index characterizing the transition to chaos.

From the map (4.1) with $a = \frac{1}{6}$ the lowest-order term in an expansion of $f(\theta)$ versus θ is of fifth order. This also leads to a complete staircase but with $D \simeq 0.81$, so the fractal dimension depends upon the nature of the inflection point. This explains the behavior of curve (c) in Fig. 10 where a is very close to $\frac{1}{6}$. We have not studied this crossover in a quantitative way. Of course, in an experimental situation one would not expect the first-order term and the third-order term to vanish simultaneously, so the generic critical exponent is $D \sim 0.87$.

Clearly, it is a *local* property of the map, namely the behavior around the inflection point which determines the fractal dimension. The behavior of the map away from the inflection point does not affect the scaling properties associated with very-high-order iterates.

We would like to stress that although the dimension was calculated by considering steps in a large interval of Ω , it is a well-defined number at any *point* on the transition line. The index D expresses the self-similarity everywhere. In principle, we could choose any infinitesimal interval $\Delta\Omega$ around this particular point and derive the scaling properties. We have checked this by investigating the scaling properties of steps in different small intervals of Ω on the critical line. If the scaling index is universal a scaling law for an interval must necessarily apply to any part of the interval. Also, in principle, the locality of the scaling behavior implies that the same scaling behavior would apply if $\Delta(P/Q)$ is considered as a function of a variable Ω' which is a smooth function of Ω . This is of importance when analyzing experiments since the effective Ω which enters the circle map is generally a complicated function of the variables in the experiment, such as currents and voltages in Josephson junctions and charge-density-wave (CDW) systems.

The transition to chaos is caused by the competition between two temporal periods. There is an analogous situation in condensed-matter physics where mode locking and chaos occur as a consequence of competition between spatial periods, namely the commensurate-incommensurate transition. In the Frenkel-Kontorowa model¹¹ and the axial next-nearest-neighbor Ising model¹² there is a competition between the lattice constant and the periods of structurally or magnetically ordered structures. The latter model has a phase diagram almost identical to Fig. 9: There is a regime with regular incommensurate ("quasi-periodic") structures between commensurate ("periodic") structures, and a regime with overlapping metastable commensurate and spatially chaotic structures, separated

(probably) by a line along which a staircase is complete. The critical properties are not universal, but depend on the actual interactions in the models,¹⁰ probably because the discrete mappings constructed from these models are Hamiltonian and not dissipative.

V. CROSSOVER BEHAVIOR FOR $K \lesssim 1$

The steps do not fill up the entire Ω axis for $K < 1$ and the slope D in the $\log_{10}N(r)$ versus $\log_{10}(1/r)$ plot must then necessarily converge towards $D=1$. In fact, when K is only slightly smaller than 1 it seems that the scaling follows $D \sim 0.87$ down to a certain scale (depending on $1-K$) and then makes a smooth crossover to the trivial scaling characterized by $D=1$. In this section we shall define and estimate the exponents characterizing this crossover, and the measure of quasiperiodic orbits for $K < 1$.

First, let us follow the consequences of treating Q as a "scaling variable" as in (3.6) and (3.7). Thus we assume that the average widths at criticality have the scaling behavior

$$\langle \Delta\Omega(Q) \rangle_P \sim Q^{-(2/D_2)}, \quad D_2 \sim D \sim 0.87.$$

A plausible scaling ansatz for $K < 1$ would be

$$\langle \Delta\Omega(Q) \rangle_P Q^{(2/D_2)} \sim \exp[-a(1-K)^\phi Q]. \quad (5.1)$$

We, therefore, plot the quantity on the left-hand side of (5.1) versus Q (Fig. 11) for 10 different values of $(1-K)$ ranging from 0.0025 to 0.1, using staircases found by means of the numerical methods of Sec. II. The linear behavior indicates that

$$\langle \Delta\Omega(Q) \rangle_P Q^{(2/D_2)} \sim \exp[-A(K)Q]. \quad (5.2)$$

Figure 12 shows $\log_{10}A(K)$ versus $(1-K)$. From the slope of the apparently straight line it seems plausible that the ansatz (5.1) indeed holds, with $\phi \sim 1$, in agreement with the nonsingular behavior of the widths of the plateaus as K approaches 1 (see Fig. 9). Somewhat surprisingly, this means that the functional form of $\Delta(P/Q)$ for

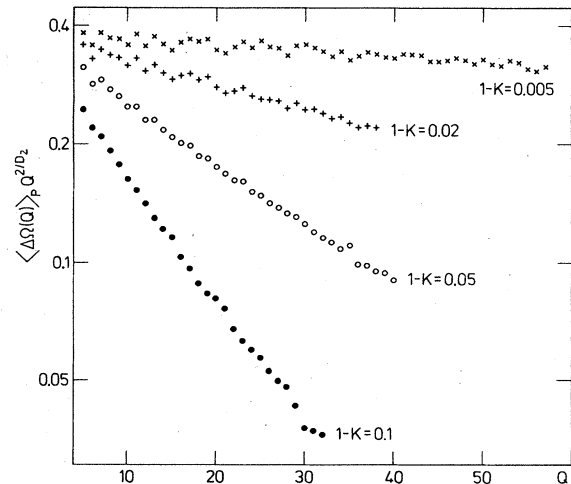


FIG. 11. Plot of $\log_{10}\langle \Delta\Omega(Q,K) \rangle_P Q^{2/D_2}$ vs Q for various values of $(1-K)$.

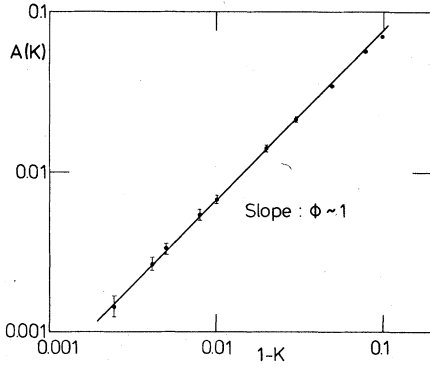


FIG. 12. Plot of $\log_{10} A(K)$ [where $A(K)$ are the slopes of the straight lines found in Fig. 11] vs $\log_{10}(1-K)$. The straight line is consistent with an exponent $\phi \sim 1$.

$K \ll 1$ is the same as for $K=1$: for small K , $\Delta(P/Q) \sim K^Q = e^{Q \ln K}$, which becomes $e^{Q(1-K)}$ for $K \sim 1$. The Arnol'd tongues grow in a uniform way from $K=0$ to $K=1$.

Equation (5.1) indicates that steps with $Q \geq 1/(1-K)$ are effectively cut off for $K < 1$, leaving room for quasi-periodic orbits. The integrated measure $M(K)$ of the support of these orbits becomes

$$M(K) = \int_{Q=1/(1-K)}^{\infty} dQ Q Q^{-2/D_2} \sim (1-K)^{\beta_2}, \quad (5.3)$$

where the exponent β obeys the scaling law

$$\beta_2 = \frac{2}{D_2} - 2 = \delta - 2 \sim 0.29. \quad (5.4)$$

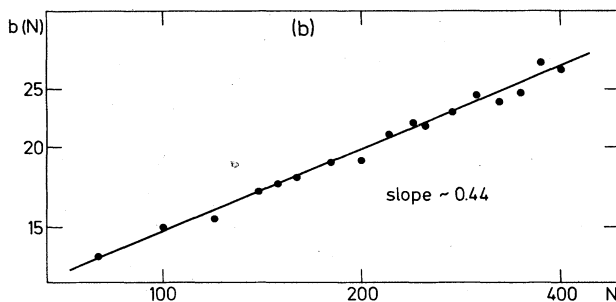
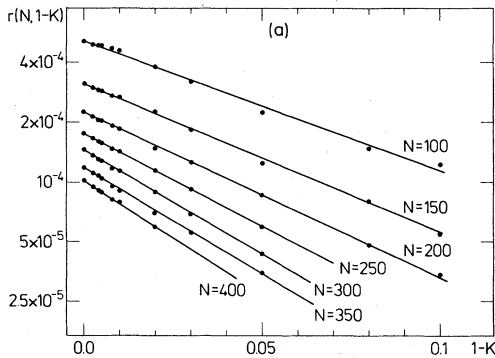


FIG. 13. (a) Scale r for which there are N intervals wider than r plotted vs $(1-K)$. (b) Plot of $\log_{10} b(N_1)$, defined by Eq. (5.5) vs $\log_{10} N_1$.

This approach seems not entirely satisfactory: there is no *a priori* reason why Q should be the natural scaling variable and thus for the scaling ansatz to make sense. The considerable spread around the straight line in Fig. 12 also points in that direction.

A more natural choice of scaling variable is the actual width of the resonances, the quantity that directly enters into the calculation of $M(K)$. Hence, for various values of $(1-K)$ we have calculated the scale $r(N_1, K)$ such that the number of resonances in the interval $[0, 1]$ which are wider than r is precisely N_1 . Obviously, this function is a decreasing function of $(1-K)$ since the intervals become narrower. Figure 13(a) shows $\log_{10} r(N_1, K)$ versus $1-K$ for several values of N_1 . The straight lines indicate exponential behavior:

$$r(N_1, K) = r(N_1, 0) \exp[-b(N_1)(1-K)]. \quad (5.5)$$

Figure 13(b) shows $\log_{10} b(N_1)$ versus $\log_{10} N_1$. The linear behavior allows us to define an exponent ν :

$$b(N_1) \sim N_1^{1/D\nu}, \quad 1/D\nu \simeq 0.44 \pm 0.02. \quad (5.6)$$

Equations (5.5) and (5.6) give a cutoff of the number of resonances, $N_0(K)$, which give a contribution to the integrated measure below criticality:

$$N_0(K) \sim (1-K)^{-D\nu}. \quad (5.7)$$

These N_0 resonances which survive below the transition are precisely those which are wider than a scale r_0 at $(1-K)=0$, with N_0 related to r_0 through Eq. (3.5), so

$$r_0 \approx (1-K)^\nu, \quad \nu \sim 2.63. \quad (5.8)$$

In other words, the plateaus which are narrower than r_0 at $K=1$ are effectively cut off at a value of $K < 1$ given by (5.8).

In a sense, $(1-K)$ plays the role of the reduced temperature near a second-order phase transition, and $1/r_0$ is the "correlation length" which diverges at the transition. The measure of the quasiperiodic orbits is a valid order parameter for the transition since it is zero above the transition and nonzero below the transition. This measure is precisely the measure of the periodic orbits which are cut off below the transition:

$$\begin{aligned} M(K) &= \int_0^{(1-K)^\nu} -\frac{\partial N_1}{\partial r} r dr \\ &\sim (1-K)^{\nu(1-D)} \\ &\equiv (1-K)^\beta, \quad \beta \sim 0.34 \pm 0.02. \end{aligned} \quad (5.9)$$

Equation (5.9) defines the scaling relation

$$D = 1 - \beta/\nu \quad (5.10)$$

which is very similar to the relation

$$D = d - \beta/\nu \quad (5.11)$$

which has been derived for second-order phase transitions. Here, d is the Euclidean dimension. The exponent β defined here seems to differ somewhat from the exponent β_2 derived from (5.4). We believe that the equation (5.11)

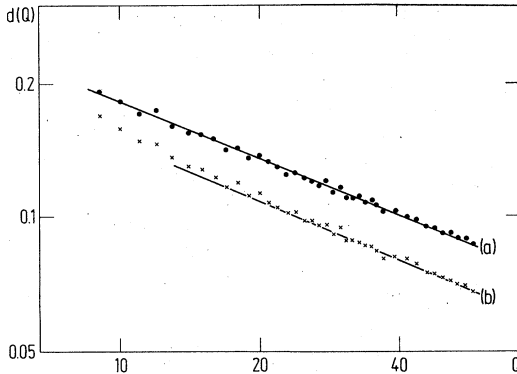


FIG. 14. Plot of $\log_{10}d(Q)$, defined by Eq. (5.5), vs $\log_{10}Q$. The slope yields an exponent $\alpha=0.421\pm 2.5\times 10^{-3}$ for $a=0$. The curve (b) is calculated for $a=-0.25$ in Eq. (4.1).

gives the proper asymptotic behavior. The expressions (5.4) and (5.11) are identical only for $\delta=\nu$. We do not believe that this relation holds; thus the result (5.4) seems to be spurious due to the use of the wrong scaling variable Q .

Besides the exponent D which characterizes the scaling in the Ω variable, we can also define a scaling index for the θ variable. For the superstable cycle of the P/Q step we find the point θ_i of the cycle $\theta_2, \dots, \theta_Q$ which is closest to zero, and define $d_1(P/Q)=\min(\theta_i, 1-\theta_i)$. For constant Q , $d_1(P/Q)$ is averaged over the numerators P :

$$d(Q)=\langle d_1(P/Q) \rangle_P, \quad (5.12)$$

and $d(Q)$ is plotted against Q on a log-log scale (Fig. 14). The straight line indicates

$$d(Q)\sim Q^{-\alpha}, \quad \alpha=0.421\pm 2.5\times 10^{-3}. \quad (5.13)$$

This number also seems to be universal as indicated by the line (b) in the figure which is based on the map (4.1) with $a=-0.25$. Our value for α is distinctly different from the corresponding value for limit cycles converging to the golden mean found by Shenker⁶ ($\alpha_G=0.527$).

The smallest distance between any two points in the cycle also scales with a power law,

$$d_{\min}(Q)=\langle d_{\min}(P/Q) \rangle_P \sim Q^{-\alpha'} \quad (5.14)$$

with $\alpha'\sim 1.58$.

VI. SCALING NEAR RATIONAL WINDING NUMBERS

Close to the instability point of the (0/1) plateau the increments in phase between two iterations, $\theta_i-\theta_{i-1}$, become infinitesimally small, and the map (1.3) may be studied in the continuum approximation, $\theta_i=\theta_{i-1}\sim d\theta/dz$:

$$\frac{d\theta}{dz}=\Omega-\frac{K}{2\pi}\sin(2\pi\theta). \quad (6.1)$$

This equation can be integrated to yield

$$\theta=\frac{1}{\pi}\tan^{-1}\left[\frac{K}{2\pi\Omega}-\frac{\omega}{\Omega}\tan(\omega\pi z)\right], \quad (6.2)$$

where

$$\omega=[\Omega^2-(K/2\pi)^2]^{1/2}.$$

This equation shows that (6.1) has a transition from periodic behavior with $W=0$ to quasiperiodic behavior with $W>0$. The critical value of Ω is $\Omega_0=(K/2\pi)$. For $\Omega\gtrsim\Omega_0$ the winding number is given by

$$W=\omega=[\Omega^2-(K/2\pi)^2]^{1/2} \\ \sim[\Omega-(K/2\pi)]^{1/2}. \quad (6.3)$$

The square-root behavior can easily be identified in Fig. 3. For the series of rational numbers $1/Q$, which converges to zero, the distance between two consecutive midpoints of intervals, $\Omega_M(Q)$ and $\Omega_m(Q+1)$, therefore scales as

$$S(Q)=\Omega_m(Q)-\Omega_m(Q+1) \\ \sim\frac{1}{Q^2}-\frac{1}{(Q+1)^2}\sim Q^{-3}. \quad (6.4)$$

By expanding around other steps such as $P/Q=\frac{1}{2}$, one finds similar square-root behavior; in fact, the square-root behavior must occur around every single step. The result (6.4) has been derived previously by Kaneko¹⁷ using a phenomenological theory.

When the staircase is complete the widths $\Delta\Omega(1/Q)$ cannot decay with an exponent which is smaller than 3,

$$\Delta\Omega(1/Q)\sim Q^{-\delta'}, \quad \delta'>3, \quad (6.5)$$

since for $\delta'<3$ there would not be sufficient room for intervals on small scales [the widths must decay at least as the difference $S(Q)$ between steps]. Figure 15 shows $\log_{10}\Delta\Omega(1/Q)$ versus $\log_{10}Q$. The asymptotic slope yields $\delta'=3$, but the convergence is rather slow. The value of the exponent δ' when approaching rational numbers is thus much bigger than the value 2.16 for rationals approaching the golden mean, and the value 2.29 for the total staircase.

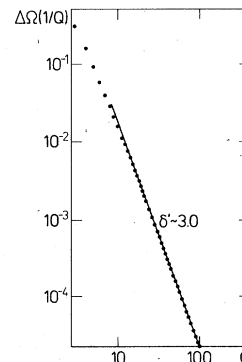


FIG. 15. Plot of $\log_{10}\Delta\Omega(1/Q)$ vs $\log_{10}Q$. The asymptotic straight line yields an exponent $\delta'=3$.

For the series $k/(2k+1)$ converging towards $\frac{1}{2}$ we find $\Delta\Omega(k/(2k+1)) \sim (2k+1)^{-3}$, and similar behavior around several other numbers such as $K/(3k+1)$: $k/(4k+1)$ converging towards rationals. In fact, the convergence seems to be exponential,¹⁸

$$\Delta\Omega(P/Q)Q^3 \sim Ae^{bQ^{-c}},$$

for these rational series, with nonuniversal constants A , b , and c .

ACKNOWLEDGMENT

We are grateful to Boris Shraiman, P. V. Christiansen, I. Satija, P. Cvitanovic, J. Doyne Farmer, M. J. Feigenbaum, J. Myrheim, and L. Glass, for stimulating discussions on circle maps. This work was supported by the Division of Materials Sciences of the U. S. Department of Energy under Contract No. DE-AC02-76CH00016 and by the Danish Natural Science Research Council. T. B. would also like to acknowledge support by National Science Foundation Grant No. DMR-83-14625.

- ¹M. J. Feigenbaum, *J. Stat. Phys.* **19**, 25 (1979); **21**, 669 (1979).
²B. V. Chirikov, *Phys. Rep.* **52**, 263 (1979).
³For an introduction see, e.g., V. I. Arnol'd, *Geometrical Methods in the Theory of Ordinary Differential Equations* (Springer, Berlin, 1982).
⁴V. I. Arnol'd, *Am. Math. Soc. Trans., Ser. 2* **46**, 213 (1965).
⁵M. R. Herman, in *Geometry and Topology*, edited by J. Palis (Springer, Berlin, 1977), Vol. 597, p. 271.
⁶S. J. Shenker, *Physica (Utrecht)* **5D**, 405 (1982).
⁷M. J. Feigenbaum, L. P. Kadanoff, and S. J. Shenker, *Physica (Utrecht)* **5D**, 370 (1982).
⁸D. Rand, S. Ostlund, J. Sethna, and E. Siggia, *Phys. Rev. Lett.* **49**, 132 (1982); *Physica (Utrecht)* **6D**, 303 (1984).
⁹M. H. Jensen, P. Bak, and T. Bohr, *Phys. Rev. Lett.* **50**, 1637 (1983).
¹⁰P. Bak and R. Bruinsma, *Phys. Rev. Lett.* **49**, 249 (1982);

- Phys. Rev. B* **27**, 5824 (1983).
¹¹S. Aubry, in *Solitons and Condensed Matter Physics*, edited by A. R. Bishop and T. Schneider (Springer, Berlin, 1979), p. 264.
¹²P. Bak and J. von Boehm, *Phys. Rev. B* **21**, 5297 (1980); M. H. Jensen and P. Bak, *ibid.* **27**, 6853 (1983).
¹³B. B. Mandelbrot, *Fractals: Form, Change, and Dimension* (Freeman, San Francisco, 1977).
¹⁴V. N. Belykh, N. F. Pedersen, and O. H. Soerensen, *Phys. Rev. B* **16**, 4860 (1977).
¹⁵S. E. Brown, G. Mozurkewich, and G. Grüner, *Phys. Rev. Lett.* **52**, 2272 (1984).
¹⁶L. Glass and R. Perez, *Phys. Rev. Lett.* **48**, 1772 (1982).
¹⁷K. Kaneko, *Prog. Theor. Phys.* **69**, 669 (1982); **69**, 403 (1983).
¹⁸B. Shraiman made us aware of this possibility.